Geometric phase effect study in electric dipole moment rings

Christian Carli* and Malek Haj Tahar
CERN, Geneva CH-1211, Switzerland

(Received 20 January 2022; accepted 16 May 2022; published 10 June 2022)

Several proposals to measure a possible small electric dipole moment (EDM) of charged particles aligned with the spin and the well-known magnetic dipole moment (MDM) are based on the concept to circulate bunches with an initial polarization in the horizontal plane and to observe the buildup of a vertical spin component caused by the EDM. Most proposals aim at operating the ring with "frozen spin," such that, with an MDM only, the spin remains aligned with the trajectory. The signature of a finite EDM is the buildup of a vertical spin component. Machine imperfections may lead as well to a vertical spin buildup, which can be misinterpreted as an EDM and thus limit the sensitivity of the experiment. For that reason, a good understanding of spin dynamics is mandatory to estimate and limit such systematic errors in the measurement. In this paper, a coordinate system attached to the trajectory is introduced to expand the spin. This is of particular interest for fully electric EDM rings operated at the "magic energy" to satisfy the frozen spin condition. The procedure is used for a straightforward analysis of geometric phase and other second order effects, which limit the possible sensitivity, i.e., the smallest EDM which can be detected in presence of systematic effects.

DOI: 10.1103/PhysRevAccelBeams.25.064001

I. INTRODUCTION

Several schemes to measure the electric dipole moment (EDM) of charged particles are discussed at present. Most of these proposals foresee to run a synchrotron satisfying the frozen spin condition. This condition requires that, in the absence of an EDM and with the well-known magnetic dipole moment (MDM) in a perfect machine, bunches with initial longitudinal polarization (parallel or antiparallel to the direction of movement) remain longitudinally polarized. This implies that the spin of a reference particle (with the reference energy and on reference orbit in the perfect machine) follows the direction of the trajectory. This is achieved by an appropriate choice of the electric and magnetic fields of bending elements [1–6]. The effect of a finite EDM is a rotation of the spin from the longitudinal direction into the vertical one. The resulting vertical spin buildup, which is very small for the smallest EDM to be detected in typical proposals, is measured with a polarimeter. The study presented here is of particular interest for a special scheme possible only for particles with positive anomalous magnetic moment $G = (g-2)/2 > 0$ such as protons: The ring is operated with beams at the magic energy, where the frozen spin condition is met with only electric fields [7–9].

Studies on the limitations of such an EDM measurement require a good understanding of the spin dynamics, in particular in a ring operated close to the frozen spin condition. The spin of different particles may rotate differently with respect to the direction of movement depending on synchrotron and betatron oscillation amplitudes; this introduces spin decoherence and limits the duration of an EDM measurement. In an imperfect machine with misaligned magnets and electrostatic guiding and focusing elements, various effects generate a vertical spin component with only an MDM. For many mechanisms, these vertical spin components cannot be disentangled from a finite EDM and, thus, lead to a systematic error in the measurement. A good understanding of the underlying effects is mandatory to estimate the sensitivity of the measurement and mitigate some of the mechanisms.

Typical tracking codes use a coordinate system attached to a reference trajectory (closed orbit of the perfect machine and design energy) both to describe trajectories and to expand a vector describing the spin. In a magic energy frozen spin ring, the spin vector of a particle is almost parallel to the direction of the movement. As a consequence, betatron oscillations will lead to oscillations of the spin vector when expanded in this coordinate system. Here a coordinate system attached to

*Christian.Carli@cern.ch

the particle trajectory, similar to the one described in [10] for magnetic rings, is introduced to expand the spin vector; as a consequence, the transverse spin components of a particle close to the frozen spin condition in a magic energy EDM ring remain small. The procedure is used to describe and analyze the so-called geometric phase and other second order effects, which limit the possible sensitivity of an EDM measurement in a magic energy frozen spin ring.

In Sec. II, the basic equations to describe the rotation of the spin and the particle direction in an electromagnetic field will be described. In Sec. III, the coordinate system attached to the trajectory and relevant angular frequencies will be introduced. Finally, the formalism is applied in Sec. IV to analyze geometric phase effects in fully electric magic energy EDM rings.

II. ANGULAR FREQUENCIES DESCRIBING THE ROTATIONS OF THE SPIN AND THE MOMENTUM AND THEIR DIFFERENCE

A. Thomas-BMT equation to describe the rotation of the particle spin

Spin rotations of charged particles with both an MDM and an EDM aligned with the particle spin are described by the Thomas-BMT equation with additional terms due to the EDM. The vector $\vec{S}$ is a unit vector describing the direction of the spin in the inertial rest frame of the particle. The time derivative of the spin direction $\vec{S}$ of a particle with charge q and mass m in a magnetic field $\vec{B}$ and an electric field $\vec{E}$ defined in the laboratory frame is given for example in [11,12] and becomes in SI units

$$\begin{aligned}
\frac{d\vec{S}}{dt} &= \vec{\Omega}_s \times \vec{S} \\
\vec{\Omega}_s &= \vec{\Omega}_{\mathrm{MDM}} + \vec{\Omega}_{\mathrm{EDM}} \\
&= -\frac{q}{m}\left[\left(G+\frac{1}{\gamma}\right)\vec{B} - G\frac{\gamma-1}{\gamma}\frac{\vec{B}\cdot\vec{\beta}}{\beta^2}\vec{\beta} - \left(G+\frac{1}{\gamma+1}\right)\vec{\beta}\times\frac{\vec{E}}{c} + \frac{\eta}{2}\left(\frac{\vec{E}}{c} - \frac{\gamma-1}{c\gamma}\frac{\vec{E}\cdot\vec{\beta}}{\beta^2}\vec{\beta} + \vec{\beta}\times\vec{B}\right)\right] \\
&= -\frac{q}{m}\left[\left(G+\frac{1}{\gamma}\right)\vec{B}_\perp + (G+1)\frac{\vec{B}_\parallel}{\gamma} - \left(G+\frac{1}{\gamma+1}\right)\vec{\beta}\times\frac{\vec{E}}{c} + \frac{\eta}{2}\left(\frac{\vec{E}_\perp}{c} + \frac{1}{\gamma}\frac{\vec{E}_\parallel}{c} + \vec{\beta}\times\vec{B}\right)\right], \qquad (1)
\end{aligned}$$

where β and γ are the relativistic factors and $\vec{\beta} = \vec{v}/c$ is a vector with length β and a direction parallel to the velocity ($\vec{v}$ and c are the velocity of the particle and the velocity of light, respectively). The quantities G and η describe the well-known magnetic moment and the EDM to be measured, respectively. For the case of protons $G = 1.79285$. Note that for a proton EDM of $d_s = 10^{-29}\ e\,\mathrm{cm}$, which is often quoted as the expected sensitivity of the currently proposed experiments, η is as low as $\eta_s = 1.9 \times 10^{-15}$. The indices $\parallel$ and $\perp$ denote the component of a vector parallel and perpendicular to the direction of movement; for example, for the electric field $\vec{E}_\parallel = (\vec{t}\cdot\vec{E})\vec{t}$ and $\vec{E}_\perp = \vec{E} - (\vec{t}\cdot\vec{E})\vec{t}$ where $\vec{t} = \vec{\beta}/\beta = \vec{p}/p$ is a unit vector pointing in the direction of the movement. $\vec{p} = \gamma m\vec{\beta}$ is the momentum vector and p is the absolute value of the momentum.

B. Angular frequency describing the change of direction of the trajectory

An angular frequency describing the rotation of the direction of the trajectory of a particle can be derived with the help of Fig. 1. The aim is to find an angular frequency $\vec{\Omega}_p$ such that the time derivative of $\vec{t}$ is given by

$$\dot{\vec{t}} = \frac{d\vec{t}}{dt} = \vec{\Omega}_p \times \vec{t}.$$

The force acting on the particle is split into a longitudinal and a perpendicular part $\vec{F} = \dot{\vec{p}}_\parallel + \dot{\vec{p}}_\perp$ with $\dot{\vec{p}}_\parallel = (\vec{t}\cdot\dot{\vec{p}})\vec{t}$. Only the component of the force $\dot{\vec{p}}_\perp$ perpendicular to the momentum changes the direction of the trajectory. The component $\dot{\vec{p}}_\parallel$ parallel to the momentum alters the particle energy, but not the direction of motion. The change in the direction of the trajectory is described by the following angular frequency perpendicular to the trajectory:

$$\begin{aligned}
\vec{\Omega}_{p,\perp} &= \frac{\vec{p}\times\dot{\vec{p}}_\perp}{p^2} = \frac{\vec{p}\times\dot{\vec{p}}}{p^2} = \frac{q}{\gamma m\beta^2}\vec{\beta}\times\left(\frac{\vec{E}}{c} + \vec{\beta}\times\vec{B}\right) \\
&= \frac{q}{\gamma m}\left(\frac{1}{\beta^2}\vec{\beta}\times\frac{\vec{E}}{c} - \vec{B}_\perp\right). \qquad (2)
\end{aligned}$$

The general expression for $\vec{\Omega}_p$ is thus given by its transverse component plus an arbitrary longitudinal component:

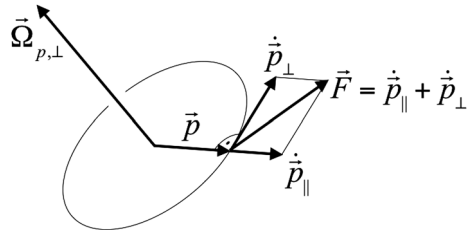

FIG. 1. Angular frequency describing the rotation of the direction of the particle trajectory.

$$\vec{\Omega}_p = \frac{q}{\gamma m}\left(\frac{1}{\beta^2}\vec{\beta}\times\frac{\vec{E}}{c} - \vec{B}_\perp\right) + \varkappa\vec{t}. \tag{3}$$

The parameter $\varkappa$ can be chosen freely. In consequence, the longitudinal component of $\vec{\Omega}_p$ and quantities depending on it have to be interpreted with care.

C. Difference between the angular frequencies describing the rotation of the spin and the rotation of the particle trajectory

The difference in the angular frequencies describing the rotation of the spin and the rotation of the direction of the particle movement, given in Eqs. (1) and (3), respectively, is:

$$\Delta\vec{\Omega} = \vec{\Omega}_s - \vec{\Omega}_p = -\frac{q}{m}\left[G\vec{B}_\perp + (G+1)\frac{\vec{B}_\parallel}{\gamma} - \left(G - \frac{1}{\gamma^2-1}\right)\vec{\beta}\times\frac{\vec{E}}{c} + \frac{\eta}{2}\left(\frac{\vec{E}_\perp}{c} + \frac{1}{\gamma}\frac{\vec{E}_\parallel}{c} + \vec{\beta}\times\vec{B}\right)\right] - \varkappa\vec{t}. \tag{4}$$

This equation has to be interpreted with care due to the undefined longitudinal component corresponding to a torsion around the direction of the movement. It can be used to derive the frozen spin condition by considering the time derivative of the longitudinal component $S_\parallel = \vec{S}\cdot\vec{t}$ given by

$$\begin{aligned}\frac{d}{dt}S_\parallel &= \frac{d}{dt}(\vec{S}\cdot\vec{t}) = \vec{S}\cdot(\vec{\Omega}_p\times\vec{t}) + (\vec{\Omega}_s\times\vec{S})\cdot\vec{t} \\ &= \vec{t}\cdot(\vec{S}\times\vec{\Omega}_p) + (\vec{\Omega}_s\times\vec{S})\cdot\vec{t} = \vec{t}\cdot(\Delta\vec{\Omega}\times\vec{S})\end{aligned}$$

which vanishes if the transverse component $\Delta\vec{\Omega}_\perp$ of the vector $\Delta\vec{\Omega}$ is zero. Thus, the frozen spin condition is fulfilled with $\Delta\vec{\Omega}_\perp = 0$. The longitudinal component of $\Delta\vec{\Omega}$ is irrelevant for the frozen spin condition.

The evolution of the spin components in a rotating coordinate system, e.g., following the design trajectory, may as well be described by an angular frequency. In this case, the rotation of the coordinate system used to expand the spin must be determined precisely. Otherwise artifacts such as the one described in Sec. II E may occur. With the coordinate system introduced in Sec. III and attached to the trajectory, the angular frequency describing the evolution of the spin components becomes $\Delta\vec{\Omega}$ with a suitable choice of the longitudinal component.

D. Recapitulation of the concepts of frozen spin and magic energy

In Sec. II C, it has been shown that the frozen spin condition is fulfilled if the orthogonal part of $\Delta\vec{\Omega}$ given in Eq. (4) vanishes. For a particle on the reference orbit in a perfect EDM ring as sketched in Fig. 2, the quantity $\Delta\vec{\Omega}_\perp$ for particle without EDM ($\eta = 0$) has only a vertical component and is given by

$$\Delta\vec{\Omega}_\perp = -\frac{q}{m}\left[GB_y - \left(G - \frac{1}{\beta^2\gamma^2}\right)\frac{\beta E_x}{c}\right]\vec{e}_y,$$

which, if set to zero, leads to the well-known condition for frozen spin:

$$B_y = \left(\frac{\beta^2\gamma^2 G - 1}{\beta^2\gamma^2 G}\right)\frac{E_x}{c}.$$

At the magic energy E_m, which exists only for particles with $G > 0$, the frozen spin condition is met with magnetic field $B_y = 0$, which leads to the following condition:

$$\beta_m\gamma_m = \frac{1}{\sqrt{G}} \quad \text{and} \quad E_m = \left(\sqrt{1+\frac{1}{G}} - 1\right)mc^2, \tag{5}$$

where the index m is used to refer to the magic energy and E_m is the (kinetic) magic energy. For protons, one obtains $\gamma_m = 1.2481$, $\beta_m = 0.5984$, $E_m = 232.8$ MeV, and $p_m = 700.7$ MeV$/c$. The concept of a magic energy proton EDM ring foresees a fully electric lattice with no magnetic element inside state-of-the-art magnetic shielding and with bunches polarized parallel to the trajectory. This allows to minimize residual magnetic fields, which are expected to lead to the dominant systematic effects limiting the sensitivity of the measurement ring.

The average electric field for a $C = 500$ m circumference proton ring is $\bar{E}_x = -5.27$ MV/m. A nonzero EDM leads to a rotation of the spin from the longitudinal direction into the vertical one as indicated by the dashed

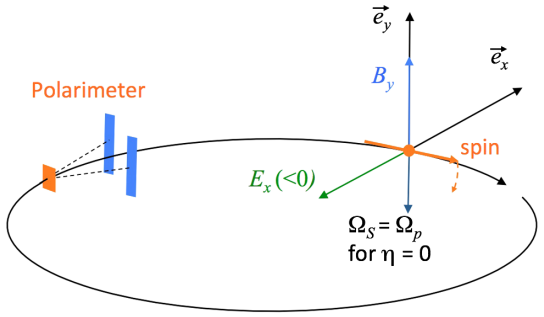

FIG. 2. Principle of a frozen spin EDM ring with a beam rotating clockwise. Note that the magnetic field $B_y > 0$ points upwards and the radial electric field $E_x < 0$ points toward the ring center as would be the case for a proton frozen spin EDM ring operated below the magic energy.

arrow in Fig. 2 and described by the radial component of the angular frequency given in Eq. (4). For an EDM of 10^{-29} e cm corresponding to $\eta = 1.9 \times 10^{-15}$, one obtains for a 500 m proton magic energy EDM ring:

$$\Delta\Omega_{x,E} = -\frac{q\eta}{2mc}\bar{E}_x = 1.6 \text{ nrad/s}. \tag{6}$$

Note that already very small imperfections, such as residual vertical magnetic fields or deviations of the bending electric fields or the rf frequency from their nominal values, will rotate the spin in the horizontal plane. Thus, a feedback system based on a measurement of the horizontal polarization is an essential ingredient of the concept.

Other essential features of the proposal are as follows: Simultaneous circulation of beams in both directions [7,8]. The reasons are (i) for the baseline fully electrostatic ring, spin rotations proportional to the average radial magnetic field and which cannot be disentangled from a finite EDM by combining observations made with the two counterrotating beams are expected to be the main limitations to the sensitivity.[1] The measurement of the orbit difference between the two counterrotating beams gives an estimate of the average radial magnetic field. The scheme is very challenging but is not further treated here; (ii) the measurement of the vertical spin buildup for both beams allows the contribution from some (but not all!) of the systematic effects to be disentangled from an EDM. An effect generating vertical spin buildup is said not to "mimic" an EDM if measurements on two counterrotating beams allow it to be disentangled from a real EDM.

Bunches with polarization in different directions: Bunches polarized parallel and antiparallel to the velocity allow to mitigate systematics related to polarimeter imperfections. Additional bunches with radial polarization allow to observe and mitigate spin rotations from the radial into the vertical direction described in Sec. IV C.

Spin feedback to keep measurement bunches longitudinally polarized: It will be impossible to adjust in advance all relevant parameters as rf frequency and electric fields of bending elements precisely enough to keep the bunches used for the measurement polarized in a longitudinal direction for the whole duration of one store. Thus, a feedback system acting on the bunches used for the measurement has to keep the radial spin component close to zero for both of the counterrotating beams. This implies the use of two independent parameters, such as the rf frequency and an additional weak vertical magnetic field.

[1]Note that the recent proposal for a hybrid ring [13,14], where electrostatic quadrupoles are replaced by magnetic ones, allows mitigating the effect. Nevertheless, residual uncontrolled magnetic fields are likely to increase other limitations.

E. Frozen spin and vertical velocity effect

In the literature, one finds often the special form of Eq. (4), which can be obtained with a suitable choice of the parameter κ:

$$\Delta\vec{\Omega}_L = -\frac{q}{m}\left[G\vec{B} - \left(G - \frac{1}{\gamma^2 - 1}\right)\vec{\beta} \times \frac{\vec{E}}{c} + \frac{\eta}{2}\left(\frac{\vec{E}}{c} + \vec{\beta} \times \vec{B}\right)\frac{\vec{E}}{c}\right]$$

with sometimes the restrictions $\beta \cdot \vec{B} = 0$ and $\beta \cdot \vec{E} = 0$. This important equation is in general applied to derive the frozen spin condition but has to be interpreted with care.

Sometimes this difference in angular frequencies is interpreted as describing the evolution of the spin components, which is in contradiction with a phenomenon first been found in tracking studies [15,16] and sometimes also referred to as the "vertical velocity effect" [14]. In fact, for magic energy particles with a vertical slope of the trajectory ($dy(s)/ds \neq 0$) inside bending elements, a radial spin component is found to be transferred into the vertical direction. On the other hand, $\Delta\vec{\Omega}_L = 0$, which implies that all three spin components of this particle inside a bending element remain constant. The reason underlying this discrepancy is that an appropriate longitudinal component has to be added to $\Delta\vec{\Omega}_L$ to obtain the angular frequency correctly describing the evolution of the three spin components.

The derivation of an angular frequency describing the evolution of the three spin components necessitates identifying the coordinate system used to expand the particle spin. Among the options are a coordinate system attached to the trajectory introduced in Sec. III and the coordinate system following radial, but not vertical betatron oscillations used in Ref. [14]. The former has the additional advantage that the variations of the spin components of a magic energy ring become small facilitating the understanding of geometric phase effects.

III. EXPANSION OF SPIN IN A COORDINATE SYSTEM FOLLOWING THE PARTICLE TRAJECTORY

In a magic energy purely electrostatic EDM measurement ring, the spin of the particle used for the measurement mainly follows the direction of the trajectory. If the particle is deflected, e.g., in a quadrupole, the change in direction of the trajectory and the change in the spin orientation are almost identical. If the spin is expanded in the coordinate system typically used by tracking programs and attached to a reference trajectory (closed orbit in a perfect machine for particles without momentum offset), betatron oscillations lead to spin oscillations dominating all other effects. The interest to develop the spin in a coordinate system following the particle trajectory as depicted in Fig. 3 is that this

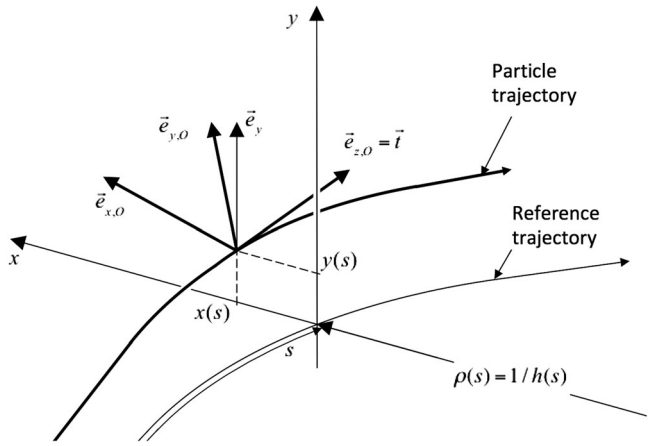

FIG. 3. Coordinate system attached to the trajectory of the particle and used to describe the spin.

main contribution to spin oscillations vanishes simplifying the understanding of subtle geometric phase effects.

A. Coordinate system

The coordinate system attached to the particle is used only to expand the spin and may still be embedded, as sketched in Fig. 3, in the standard coordinate system attached to a reference orbit. The longitudinal unit vector is the tangential vector to the trajectory $\vec{e}_{z,O} = \vec{t}$. A horizontal unit vector is introduced such that it has no vertical component with the help of the vertical unit vector $\vec{e}_y$ (perpendicular to the theoretical midplane of the synchrotron) as

$$\vec{e}_{x,O} = \frac{\vec{e}_y \times \vec{e}_{z,O}}{|\vec{e}_y \times \vec{e}_{z,O}|} = \frac{\vec{e}_y \times \vec{t}}{a_c} \tag{7}$$

with $a_c = \sqrt{1 - a_s^2}$ and $a_s = \vec{e}_y \cdot \vec{t}$. The third unit vector is given by

$$\vec{e}_{y,O} = \vec{e}_{z,O} \times \vec{e}_{x,O} = \frac{\vec{t} \times (\vec{e}_y \times \vec{t})}{a_c} = \frac{\vec{e}_y - a_s \vec{t}}{a_c}. \tag{8}$$

The next step is to derive an angular frequency $\vec{\Omega}_O$ describing the rotation of this coordinate system, such that $d\vec{e}_{i,O}/dt = \vec{\Omega}_O \times \vec{e}_{i,O}$ with i standing for x, y, or z. The transverse component of $\vec{\Omega}_O$ is given by $\vec{\Omega}_{p,\perp}$ given in Eq. (2) (fixed to give the correct time derivative of $\vec{e}_{z,O} = \vec{t}$). Thus, $\vec{\Omega}_O$ is given by the angular frequency describing the rotation of the momentum given in Eq. (3) with an appropriately chosen value for $\varkappa$, which is rewritten as

$$\vec{\Omega}_O = \vec{\Omega}_{p,\perp} + \varkappa \vec{t}$$

The easiest way to determine $\varkappa$ is to consider the vertical component of the time derivative of $\vec{e}_{x,O}$, which has to vanish by definition:

$$\frac{d(\vec{e}_{x,O} \cdot \vec{e}_y)}{dt} = \frac{d\vec{e}_{x,O}}{dt} \cdot \vec{e}_y = (\vec{\Omega}_{p,\perp} \times \vec{e}_{x,O}) \cdot \vec{e}_y + \varkappa(\vec{t} \times \vec{e}_{x,O}) \cdot \vec{e}_y = (\vec{e}_{x,O} \times \vec{e}_y) \cdot \vec{\Omega}_{p,\perp} + \varkappa \vec{e}_{y,O} \cdot \vec{e}_y = 0.$$

Making use of $\vec{e}_{x,O} \times \vec{e}_y = (\vec{t} - a_s \vec{e}_y)/a_c$ and $\vec{e}_{y,O} \cdot \vec{e}_y = a_c$, which can be derived from Eqs. (7) and (8), one obtains

$$\varkappa = -\frac{(\vec{t} - a_s \vec{e}_y) \cdot \vec{\Omega}_{p,\perp}}{a_c^2} = \frac{a_s}{a_c^2} \vec{e}_y \cdot \vec{\Omega}_{p,\perp} = \frac{a_s}{a_c^2} \Omega_{p,\perp,y}$$

and

$$\vec{\Omega}_O = \vec{\Omega}_{p,\perp} + \frac{a_s}{a_c^2} \Omega_{p,\perp,y} \vec{e}_{z,O}. \tag{9}$$

B. Expansion of the spin

The spin components expanded in the coordinate system attached to the trajectory are given by

$$\vec{S}_O = \begin{pmatrix} S_{x,O}(t) \\ S_{y,O}(t) \\ S_{z,O}(t) \end{pmatrix} = \begin{pmatrix} \vec{S}(t) \cdot \vec{e}_{x,O} \\ \vec{S}(t) \cdot \vec{e}_{y,O} \\ \vec{S}(t) \cdot \vec{e}_{z,O} \end{pmatrix}. \tag{10}$$

The time derivative of the component $S_{i,O}$ with i standing for x, y, or z is given by

$$\begin{aligned} \frac{dS_{i,O}}{dt} &= \frac{d(\vec{S} \cdot \vec{e}_{i,O})}{dt} = (\vec{\Omega}_s \times \vec{S}) \cdot \vec{e}_{i,O} + \vec{S} \cdot (\vec{\Omega}_O \times \vec{e}_{i,O}) \\ &= [(\vec{\Omega}_s - \vec{\Omega}_O) \times \vec{S}] \cdot \vec{e}_{i,O} = (\Delta\vec{\Omega}_O \times \vec{S}) \cdot \vec{e}_{i,O} \end{aligned}$$

with $\Delta\vec{\Omega}_O = \vec{\Omega}_s - \vec{\Omega}_O$. Thus, the time derivatives of the components of the spin vector expanded in the coordinate system just introduced can be computed with a simple cross product. All vectors have to be computed using this coordinate system. Using Eqs. (1) and (9) one obtains

$$\Delta\vec{\Omega}_O = \begin{pmatrix} (\vec{\Omega}_s - \vec{\Omega}_{p,\perp}) \cdot \vec{e}_{x,O} \\ (\vec{\Omega}_s - \vec{\Omega}_{p,\perp}) \cdot \vec{e}_{y,O} \\ \vec{\Omega}_s \cdot \vec{e}_{z,O} - (a_s/a_c^2)\Omega_{p,\perp,y} \end{pmatrix} = \begin{pmatrix} -\frac{q}{m}[GB_{O,x} + (G - \frac{1}{\gamma^2-1})\frac{\beta E_{O,y}}{c} + \frac{\eta}{2}(\frac{E_{O,x}}{c} - \beta B_{O,y})] \\ -\frac{q}{m}[GB_{O,y} - (G - \frac{1}{\gamma^2-1})\frac{\beta E_{O,x}}{c} + \frac{\eta}{2}(\frac{E_{O,y}}{c} + \beta B_{O,x})] \\ -\frac{q}{m}[(G+1)\frac{B_{O,z}}{\gamma} + \frac{\eta}{2}\frac{E_{O,z}}{c\gamma}] + \frac{a_s}{a_c^2}\frac{q}{m}(\frac{1}{\gamma}B_{O,y} - \frac{1}{\beta\gamma}\frac{E_{O,x}}{c}) \end{pmatrix}. \quad (11)$$

Note that the equations derived so far are exact and apply for any EDM ring using magnetic and/or electric fields. The approach is of particular interest for magic energy electric EDM rings, for which it will be applied in the next section.

IV. APPLICATION TO SECOND ORDER EFFECTS IN A MAGIC ENERGY EDM RING

Any effect generating a vertical spin other than an EDM is a source of systematic error in the measurement and thus a limitation for the sensitivity of the experiment. The formalism developed in Sec. III will be applied for analysis of systematic errors of magic energy EDM rings. The only imperfection, i.e., deviation from the ideal machine, leading to vertical spin buildup in the first order, i.e., proportional to the perturbation, is a residual average radial magnetic field,[2] which will not be treated here.

Second order effects, where in general two machine imperfections contribute to a vertical spin buildup, also have the potential to limit the sensitivity of proposed magic energy proton EDM rings. The formalism developed in Sec. III turns out to be particularly suitable for this analysis. A few simple, special configurations leading to second order effects generating vertical spin will be presented and allow us to understand some of the basic mechanisms. These can be used to estimate vertical spin buildup in a realistic lattice, which then can be compared with tracking studies.

In this analysis, it is assumed that a feedback system, as mentioned at the end of Sec. II D, will be used to ensure that the radial spin component at the location of the polarimeter remains constant. Only in the case of a perfect setup will the radial spin component at the polarimeter vanish. The EDM of the particle is also assumed to be null (setting $\eta = 0$ in Eq. (1) and all expressions derived from it). Betatron oscillations are neglected with the analysis restricted to particles following the closed orbit.

Although the general equations given are valid for any magic energy charged particle EDM ring, numerical evaluations are performed for the proton EDM lattice proposal of [20] used for most recent reports on proton EDM rings, e.g., Ref. [8].

[2]Gravity generates spin rotations proportional to the gravitational force [17–19] and, thus, can be considered as well as a first order systematic effect. However, the effects due to gravity do not mimic a finite EDM and can be predicted.

A. Orbit perturbations in both transverse planes due to misaligned quadrupoles

A special case with two quadrupoles with misalignments in both planes and at opposite positions of the ring as indicated in Fig. 4 is considered. As a concrete example and for numerical evaluations, the lattice described in [20] with quadrupole offsets as indicated and resulting horizontal and vertical orbit perturbations x_{co} and y_{co} plotted in Fig. 4 are used. Due to the horizontal orbit perturbations and the electric potentials, the kinetic energy of the particles inside bending elements is no longer magic.[3] In the first order, the relativistic gamma of a particle inside a bend is given by

$$\gamma = \gamma_m + \frac{x_{co} q E_x}{mc^2} = \gamma_m - \frac{\beta_m^2 \gamma_m}{\rho} x_{co}.$$

The vertical component of $\Delta\vec{\Omega}_O$, defined in Eq. (11), can be approximated in first order by the vertical component of $\Delta\vec{\Omega}$ given in Eq. (4) with $\varkappa = 0$ and becomes

$$\Delta\Omega_{O,y} \approx \frac{q}{m}\left(G - \frac{1}{\gamma^2 - 1}\right)\frac{\beta E_x}{c} \approx \frac{2\beta_m c}{\gamma_m}\frac{x_{co}}{\rho^2}. \quad (12)$$

For a particle with a polarization mainly in the direction parallel to the trajectory ($S_{O,z} \approx 1$), the small radial spin component as a function of the longitudinal position is approximately given by

$$S_{O,x}(\hat{s}) \approx \frac{1}{\beta_m c}\int^s d\hat{s}\,\Delta\Omega_{O,y}(\hat{s}) = \frac{2}{\gamma_m}\int^s d\hat{s}\,\frac{x_{co}(\hat{s})}{\rho^2(\hat{s})}. \quad (13)$$

The longitudinal component of $\Delta\vec{\Omega}_O$ given in Eq. (11) features a contribution from the angular frequency $\vec{\Omega}_s$ describing the rotation of the spin vector caused by a residual magnetic field component parallel to the trajectory, which vanishes for the case described, and an additional component describing a rotation of the coordinate system (torsion) around the longitudinal axis given by

$$\Delta\Omega_{O,z} = -\frac{a_s}{a_c^2}\Omega_{p,\perp,y} \approx y'_{co}\frac{\beta_m c}{\rho}, \quad (14)$$

[3]This is also the case for quadrupoles but does not lead to a vertical spin buildup in the second order of the perturbations.

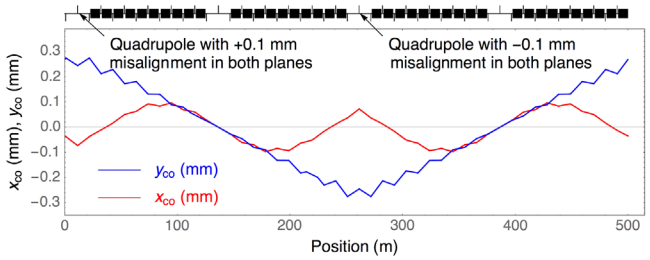

FIG. 4. Vertical and horizontal closed orbit with two quadrupole misaligned by 100 μm in both planes.

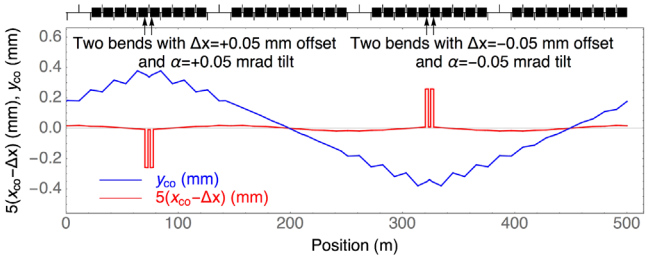

FIG. 6. Vertical and horizontal closed orbit with two pairs of bending elements with a horizontal offset of ± 50 μm and a tilt (rotation around the longitudinal axis) of ± 50 μrad.

where only terms proportional to the perturbation are kept as this is sufficient for estimates of second order effects. The resulting (average) vertical spin build-up rate is given by

$$\dot{S}_{y,O} = \frac{\beta_m c}{C}\int_0^C \frac{ds}{\beta_m c}\Delta\Omega_{O,z}(s)S_{O,x}(s) = \frac{1}{C}\int_0^C ds\frac{\beta_m c}{\rho(s)}y'_{co}(s)S_{O,x}(s) \tag{15}$$

with C the circumference. The radial spin component and derivative of the vertical closed orbit are plotted in Fig. 5 for the case described. Evaluating numerically the integral in Eq. (15), one obtains for this special case with small misalignments an average vertical spin buildup of $\dot{S}_{O,y} = -4.5$ μrad/s, which is more than three orders of magnitude larger than the one expected for the smallest EDM to be detected.

However, the effect does not mimic EDM. It can, at least in principle, be disentangled from an EDM combining results of measurements done with counterrotating beams.

B. Bending elements with horizontal offsets and tilts

A slightly more complicated case described here is a lattice with electrostatic bends displaced horizontally and tilted around the longitudinal axis. To describe the mechanism, the lattice described in [20] with two pairs of bending elements at opposite locations in the ring is used. The bending element misalignments and resulting horizontal and vertical closed orbit deformations x_{co} and y_{co} are shown in Fig. 6. In addition to the effect described in section IV A, there is a direct rotation of the spin from the longitudinal direction into the vertical one.

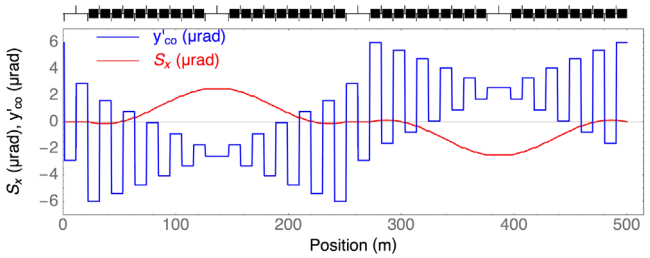

FIG. 5. Radial spin and slope of vertical closed orbit with closed orbits shown in Fig. 4 due to misaligned quadrupoles.

Due to the horizontal offset of the bending elements, the kinetic energy of the particle is different from the magic energy and, together with the vertical electric field due to the tilt, leads to a finite $\Delta\Omega_{O,x}$. The relativistic gamma of a particle inside bending elements is given by

$$\gamma = \gamma_m + \frac{qE_x}{mc^2}(x_{co}-\Delta x) = \gamma_m - \frac{\beta_m^2\gamma_m}{\rho}(x_{co}-\Delta x),$$

where Δx is the horizontal misalignment of the bending element. The resulting horizontal component of $\Delta\vec{\Omega}_O$ is

$$\Delta\Omega_{O,x} \approx -\frac{q}{m}\left(G-\frac{1}{\gamma^2-1}\right)\frac{\beta E_{O,y}}{c} \approx -\frac{2\beta_m c}{\gamma_m}\frac{(x_{co}-\Delta x)\alpha}{\rho^2}.$$

Extrapolating from Eq. (13), the small radial spin component for a particle mainly polarized parallel to its trajectory as a function of the longitudinal position is given by

$$S_{O,x}(s) = \frac{2}{\gamma_m}\int^s d\hat{s}\frac{(x_{co}(\hat{s})-\Delta x(\hat{s}))}{\rho^2(\hat{s})}. \tag{16}$$

Summing both contributions, the direct rotation from the longitudinal to the vertical direction described by $\Delta\Omega_{O,x}$ and the rotation of the radial spin component $S_{O,x}$ to the vertical direction described by $\Delta\Omega_{O,z}$ given in Eq. (14), the small average vertical spin build-up rate for a particle mainly polarized parallel to its trajectory is given by

$$\dot{S}_{O,y} = \frac{1}{C}\left[-\int_0^C ds\Delta\Omega_{O,x}(s) + \int_0^C ds\Delta\Omega_{O,z}(s)S_{O,x}(s)\right] = \frac{\beta_m c}{C}\left[\frac{2}{\gamma_m}\int_0^C ds\frac{(x_{xo}-\Delta x)\alpha}{\rho^2} + \int_0^C ds\frac{y'_{co}}{\rho}S_{O,x}\right].$$

The functions needed for numerical evaluations of the first integral are plotted in Fig. 7. Numerical evaluations of the first and second integral give contributions to $\dot{S}_{O,y}$ of -5.8

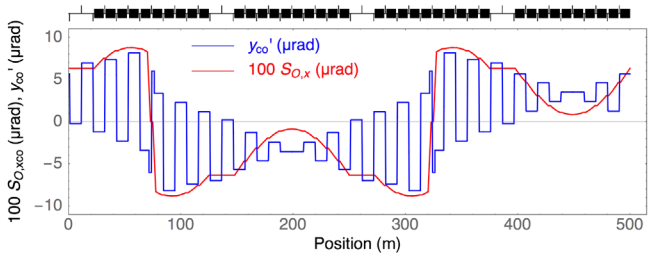

FIG. 7. Radial spin and slope of vertical closed orbit with bending element misalignments and resulting orbit distortions shown in Fig. 6.

and -0.3 μrad/s. Thus, for the special case used for numerical evaluations, the direct rotation of the spin from the longitudinal to the vertical direction dominates.

Again, the effect does not mimic EDM in the sense that it can be disentangled from an EDM by combining the results of measurements performed on counterrotating beams.

C. Nonvanishing (average) horizontal spin component and vertical slope inside bending elements

In case of imperfections of the polarimeter, an (average) horizontal spin may be present even with a feedback system in place to cancel it. A slope of the vertical closed orbit y'_{co} rotates this radial spin component into the vertical direction by the mechanism described in Sec. IV A even without spin rotations from the longitudinal direction to the radial direction. With the angular frequency describing the spin rotation around the longitudinal axis from Eq. (14), the (average) vertical spin build-up rate is given by

$$\dot{S}_{y,O} = \frac{2\pi \bar{y}'_{co} \beta_m c}{C} \mathrm{sgn}(\rho) S_{x,O}$$

with $\bar{y}'_{co}$ the average slope of the vertical closed orbit inside bending elements and $\mathrm{sgn}(\rho)$ the sign of the bending radius (positive for a clockwise beam and negative for a counterclockwise beam). Figure 8 shows the vertical closed orbit due to the misalignment by 0.1 mm of one single quadrupole of the lattice described in [20]. The resulting average slope in the bending elements is $\bar{y}'_{co} = -82$ nrad. With an average radial spin of $S_{x,O} = 1$ mrad, this leads to a vertical spin buildup of $\dot{S}_{y,O} = -0.18$ mrad/s.

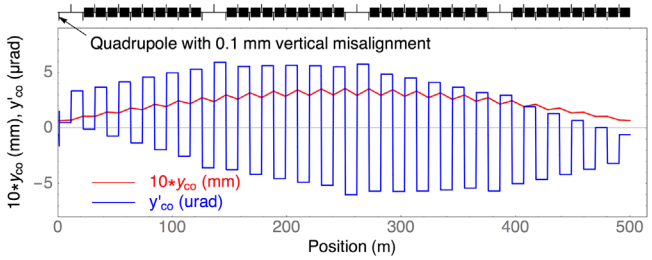

FIG. 8. Vertical closed orbit and its derivative with one quadrupole misaligned by 100 μm.

The effect may mimic a finite EDM. Contributions from counterrotating beams on the final result cancel only for the special case where (i) the absolute of the average radial spin is the same for the CW and CCW beam; (ii) the horizontal spin points toward the inside of the ring for one beam and the outside for the other. In general, with different radial polarization of the two counterrotating beams, the effect cannot be disentangled from a finite EDM. Simultaneous circulation of bunches polarized parallel and antiparallel to the trajectory may be a possible mitigation measure for this effect. Bunches with radial polarization allow to observe spin rotations around the longitudinal direction, which may be used for mitigation schemes.

D. Residual vertical magnetic fields and vertical offsets of quadrupoles

Vertical magnetic fields generate radial spin components due to direct rotation of the spin (at the location of the perturbations) and orbit distortions altering the energy in bending elements. Vertical offsets of quadrupoles (or other sources for vertical electric fields such as tilts of bendings) generate vertical closed orbit perturbations and a rotation of the radial spin into the vertical direction. The perturbations and the resulting closed orbit for the special case considered here are shown in Fig. 9.

Both the vertical magnetic field components and the electric potential due to the horizontal orbit distortions inside bending elements contribute to the generation of a small horizontal spin component. Extrapolating from Eq. (12), describing the contribution from the orbit distortion, and adding the contribution from the vertical magnetic field, the vertical component of the angular frequency $\Delta\vec{\Omega}_O$ is

$$\Delta\Omega_{O,y} \approx \frac{2\beta_m c}{\gamma_m} \frac{x_{co}}{\rho^2} - \frac{q}{m} B_{O,y}. \tag{17}$$

The small radial spin component for particles with a predominant polarization parallel to the trajectory is given by

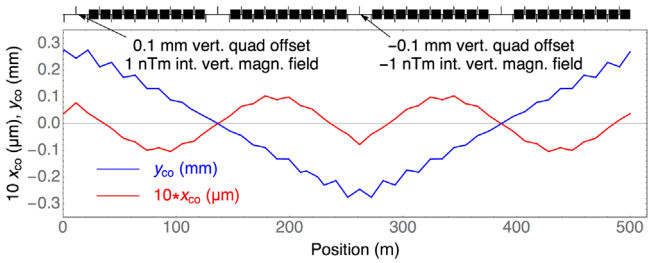

FIG. 9. Vertical and horizontal closed orbit where two opposite positions in the ring have vertical magnetic fields and vertical quadrupole offsets.

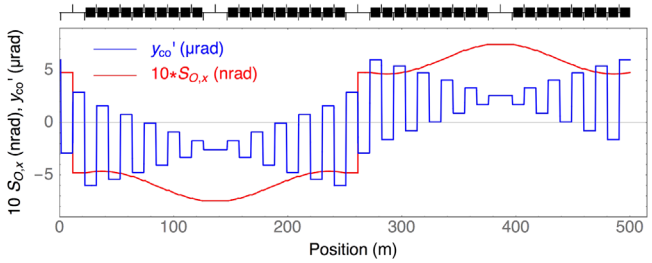

FIG. 10. Radial spin and slope of vertical closed orbit with two opposite positions in the ring with vertical magnetic fields and vertical quadrupole offsets as indicated in Fig. 9.

$$S_{O,x}(s) = \int^{s} d\hat{s}\left(\frac{2\beta_m c}{\gamma_m}\frac{x_{co}(\hat{s})}{\rho^2(\hat{s})} - \frac{q}{m}B_{O,y}(\hat{s})\right).$$

The (average) vertical buildup due to a rotation around the longitudinal direction is described by Eq. (15) derived in Sec. IV A. The functions needed to evaluate this integral are plotted in Fig. 10. The resulting (average) vertical spin build-up rate for the case described is $\dot{S}_{O,y} = 3.1$ nrad/s, which is almost twice the value expected with an EDM of $d_s = 10^{-29}\ e$ cm.

The effect described here does mimic an EDM. It is not possible to disentangle the resulting vertical spin buildup from the one generated by a finite EDM.

V. SUMMARY AND OUTLOOK

An analysis of the meaning of the difference $\Delta\vec{\Omega}$ between the angular frequencies describing the rotation of the spin $\vec{\Omega}_s$ and the rotation of the direction of movement $\vec{\Omega}_p$ has been presented. The longitudinal component is not uniquely defined and has to be interpreted with care. The transverse component of $\Delta\vec{\Omega}$ is useful to derive the frozen spin condition. A special coordinate system attached to the particle trajectory has been introduced to expand the spin. The rotation of this coordinate system is described by an angular frequency $\vec{\Omega}_O$ with a transverse component identical to the transverse component of $\vec{\Omega}_p$ and a longitudinal component, which is well defined and, in general, small.

The coordinate system attached to the trajectory introduced to expand the spin is of particular interest for electrostatic EDM rings operating at the magic energy to fulfill the frozen spin conditions. With this coordinate system, spin oscillations following the direction of the particle (approximately given by x' and y') vanish and only smaller terms remain. As a consequence, geometric phase effects can be described in a straightforward manner. In particular, a rotation of a radial spin component into the vertical direction, already seen in tracking studies [15,16], is obtained in a straightforward manner.

The spin feedback system mentioned at the end of Sec. II D to keep the radial polarization of bunches used for the measurement small generates slow spin rotations around the vertical axis. The main impact will be slow variations of the radial spin component, such that $S_{x,O}$ used in Sec. IV C, is not constant anymore. The effect can still be described by the same approach simply by replacing $S_{x,O}$ with an average value. Geometric phase effects occur at orders of magnitude faster time scales and are not affected by small changes in the radial spin component.

Several cases of "second order effects," where two deviations from the ideal design lead to vertical spin buildup, are described. Special cases not yet described in the literature are bending elements with simultaneous tilt around the longitudinal axis and a horizontal offset described in Sec. IV B and a combination of vertical magnetic fields and vertical offsets of electrostatic quadrupoles described in Sec. IV D. For the moment, second order and, in particular, geometric phase effects are described for special configurations allowing us to understand the underlying mechanisms. An important feature of such effects is whether the mimic EDM, i.e., cannot be disentangled from a real EDM by circulating simultaneously clockwise and counterclockwise beams and having bunches polarized in both beam direction and opposite to it. Without mitigation measures, some of the effects, that do not mimic EDM, generate vertical spin build-up rates several orders of magnitude larger than the ones expected with an EDM of $d_s = 10^{-29} e \cdot$ cm. Furthermore, only particles following the closed orbit have been considered and betatron oscillations have been neglected.

Several of the effects described are relevant as well for the hybrid ring proposal [13,14], where electrostatic quadrupoles are replaced by magnetic ones. An example is the spin rotations caused by bending elements with tilts around the longitudinal axis and a horizontal offset. The main effect will occur as well in hybrid rings, even though the derivations have to be adapted to this case. The main feature of hybrid rings is the disappearance of spin rotations proportional to the average radial magnetic field, which cannot be disentangled from the ones caused by a finite EDM and are the most stringent limitation to the sensitivity of a fully electrostatic magic energy EDM ring. On the other hand, with magnetic quadrupoles and sextupoles, unwanted magnetic fields are likely to increase and enhance second and higher order effects. Methods developed in this paper will help in the understanding of these effects and the resulting limitations.

The next steps for a better quantitative understanding of systematic effects and sensitivity limitations, for both the standard electrostatic and the hybrid magic energy EDM ring, require (i) studies of lattices with more realistic imperfections such as random misalignments of all quadrupoles and/or residual magnetic fields around the circumference and (ii) first order effects to be taken into account, which may be the dominant limitation. Beam based methods (already applied at the magnetic COSY ring

[21,22] in the frame of studies for charged particle EDM measurements) as quadrupole strength modulations to measure the offset between the closed orbit and quadrupoles and orbit response measurements to refine the optics model should be taken into account as mitigation measures. The generalization of the expressions given in this report to more realistic rings will then be compared with tracking results to identify the dominating systematic effects.

[1] Y. Semertzidis, A new experiment for an electric dipole moment of muon at the 10^{-24}e × cm level, in *Proceedings of Workshop on Frontier Tests of Quantum Electrodynamics and Physics of the Vacuum, Sandansky, Bulgaria, 1998*, https://cds.cern.ch/record/357718.

[2] I. B. Khriplovich, Feasibility of search for nuclear electric dipole moments at ion storage rings, Phys. Lett. B **444**, 98 (1998).

[3] F. J. M. Farley, K. Jungmann, J. P. Miller, W. M. Morse, Y. F. Orlov, B. L. Roberts, Y. K. Semertzidis, A. Silenko, and E. J. Stephenson, New Method of Measuring Electric Dipole Moments in Storage Rings, Phys. Rev. Lett. **93**, 052001 (2004).

[4] Y. Senichev, S. Andrianov, A. Ivanov, S. Chekmenev, M. Berz, and E. Valetov, Investigation of Lattice for Deuteron EDM Ring, in *Proceedings of the 12th International Computational Accelerator Physics Conference (ICAP2015), Shanghai, China* (JACoW, Geneva, Switzerland, 2016), MODBC4.

[5] A. A. Skawran and A. Lehrach, Spin tracking for deuteron EDM storage ring, J. Phys. Conf. Ser. **874**, 012050 (2017).

[6] A. Aksentev and Y. Senichev, Frequency domain method of the search for the electric dipole moment in a storage ring, J. Phys. Conf. Ser. **1435**, 012026 (2020).

[7] V. Anastassopoulos *et al.*, A proposal to measure the proton electric dipole moment with $10^{-29}e \cdot$cm sensitivity, https://www.bnl.gov/edm/files/pdf/proton_EDM_proposal_20111027_final.pdf.

[8] V. Anastassopoulos *et al.*, A storage ring experiment to detect a proton electric dipole moment, Rev. Sci. Instrum. **87**, 115116 (2016).

[9] F. Abusaif *et al.*, Storage ring to search for electric dipole moments of charged particles—Feasibility study, Report No. CERN-2021-003.

[10] E. D. Courant, Revised spin motion equations, Report No. BNL note C-A/AP/#292, 2009.

[11] D. F. Nelson, A. A. Schupp, R. W. Pidd, and H. R. Crane, Search for an Electric Dipole Moment of the Electron, Phys. Rev. Lett. **2**, 492 (1959).

[12] T. Fukuyama and A. J. Silenko, Derivation of generalized Thomas-Bargmann-Michel-Telegdi equation for a particle with electric dipole moment, Int. J. Mod. Phys. A **28**, 1350147 (2013).

[13] S. Haciomeroglu and Y. Semertzidis, Hybrid ring design in the storage-ring proton electric dipole moment experiment, Phys. Rev. Accel. Beams **22**, 034001 (2019).

[14] Z. Omarov, H. Davoudiasl, S. Hacıömeroğlu, V. Lebedev, W. M. Morse, Y. K. Semertzidis, A. J. Silenko, E. J. Stephenson, and R. Suleiman, Comprehensive symmetric-hybrid ring design for a proton EDM experiment at below $10^{-29}e$ cm, Phys. Rev. D **105**, 032001 (2022).

[15] S. Haciomeroglu, Quad misplacement studies for the pEDM rings, in *Proceedings of the CPEDM meeting* (2018), https://indico.cern.ch/event/712735/contributions/2957368/.

[16] S. Haciomeroglu and Y. K. Semertzidis, Systematic errors related to quadrupole misplacement in an all-electric storage ring for proton EDM experiment, arXiv:1709.01208.

[17] Y. N. Obukhov, A. J. Silenko, and O. V. Teryaev, Manifestations of the rotation and gravity of the Earth in high-energy physics experiments, Phys. Rev. D **94**, 044019 (2016).

[18] Y. Orlov, E. Flanagan, and Y. Semertzidis, Spin rotation by Earth's gravitational field in a frozen-spin ring, Phys. Lett. A **376**, 2822 (2012).

[19] A. Laszlo and Z. Zimboras, Quantification of GR effects in muon $(g-2)$, EDM and other spin precession experiments, Classical Quantum Gravity **35**, 175003 (2018).

[20] V. Lebedev, Accelerator physics limitations on an EDM ring design—Comments to the BNL proposal from 2011, various version of slides and a recent one at http://collaborations.fz-juelich.de/ikp/jedi/public_files/usual_event/AccPhysLimitationsOnEDMring.pdf.

[21] V. Ponzca and A. Lehrach, Simulation model improvements at the Cooler Synchrotron COSY using the LOCO Algorithm, in *Proceedings of the 12th International Particle Accelerator Conference (IPAC-2021), Campinas, SP, Brazil* (JACoW, Geneva, Switzerland), pp. 4111–4114, THPAB177.

[22] T. Wagner *et al.*, Beam-based alignment at the Cooler Synchrotron COSY as a prerequisite for an electric dipole moment measurement, J. Instrum. **16**, T02001 (2021).